Light scattering from electronic and magnetic excitations in α'-NaV$_2$O$_5$

M J Konstantinović†, K Ladavac†, A Belić†, Z V Popović†, A N Vasil'ev‡,
M Isobe§ and Y Ueda§

† Institute of Physics, PO Box 57, 11001 Belgrade, Yugoslavia
‡ Low Temperature Physics Department, Moscow State University, 119899 Moscow, Russia
§ Institute for Solid State Physics, The University of Tokyo, 7-22-1 Roppongi, Minato-ku, Tokyo
106, Japan

Abstract. We present the Raman scattering spectra of α'-NaV$_2$O$_5$ single crystal. In the high-temperature phase, besides phonon modes, there are three broad continuum-like features observed at energies centred at 160, 603 and 2400 cm^{-1} ($T = 100$ K) which are described as an indication of d–d electronic transitions of V ions. Due to the magnetic ordering at $T < 34$ K, appearing as a consequence of charge ordering, these paramagnetic bands split into several excitons with energies of 65, 106, 200, 2000 and 3000 cm^{-1}. The assigning of the lowest-energy mode at 65 cm^{-1} as the one-magnon mode, as well as the onset of the magnetic continuum at 126 cm^{-1}, is done on the basis of Monte Carlo calculation of excited states of a Heisenberg dimerized Hamiltonian without frustration. A good agreement between the measured and calculated magnetic excitation energies for $\delta = 0.047$ and $J = 455$ K has been found. Other lines in the low-temperature Raman spectra represent phonons becoming Raman active due to the Brillouin-zone-folding effect.

1. Introduction

It has recently been shown [1] that sodium vanadium oxide is a second example of an inorganic spin–Peierls compound. As for CuGeO$_3$ [2], a strong decrease of the susceptibility $\chi(T)$ in α'-NaV$_2$O$_5$ is found below $T \simeq 34$ K and described as indicating the opening of a spin gap. Lattice dimerization and the existence of the spin gap are also confirmed by x-ray, inelastic neutron scattering [3], nuclear magnetic resonance (NMR) [4] and electron spin resonance (ESR) [5] measurements. Using these techniques, the spin gap was estimated to be in the range from 85 to 98 K. Previously published infra-red [6, 7] and Raman [8, 9] spectra show the appearance of new modes below the transition temperature, but no discussion of their origin was given. Moreover, the nature of the phase transition is currently under debate, since several experimental observations have not been in accordance with the standard spin–Peierls scenario.

On the basis of an early measurement of the NaV$_2$O$_5$ crystal structure [10], it has been shown that this oxide, grown in single-crystalline form under ambient conditions, has an orthorhombic unit cell with parameters $a = 1.1318$ nm, $b = 0.3611$ nm, $c = 0.4797$ nm, $Z = 2$ and the space group $P2_1mn$ (D$_{2v}^7$). Such a crystalline structure assumes two kinds of vanadium chain along the b-axis: one consisting of magnetic V^{4+} ions ($S = 1/2$ chains) and the other of non-magnetic V^{5+} ions ($S = 0$ chains). These chains are aligned parallel to each other and share an edge of adjacent VO$_5$ pyramids, thus forming layers in an ab-plane. Na
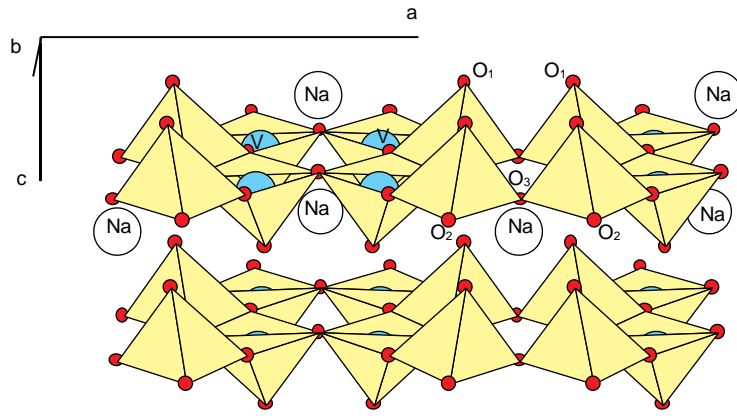
Figure 1. A schematic representation of the α'-NaV$_2$O$_5$ crystal structure.
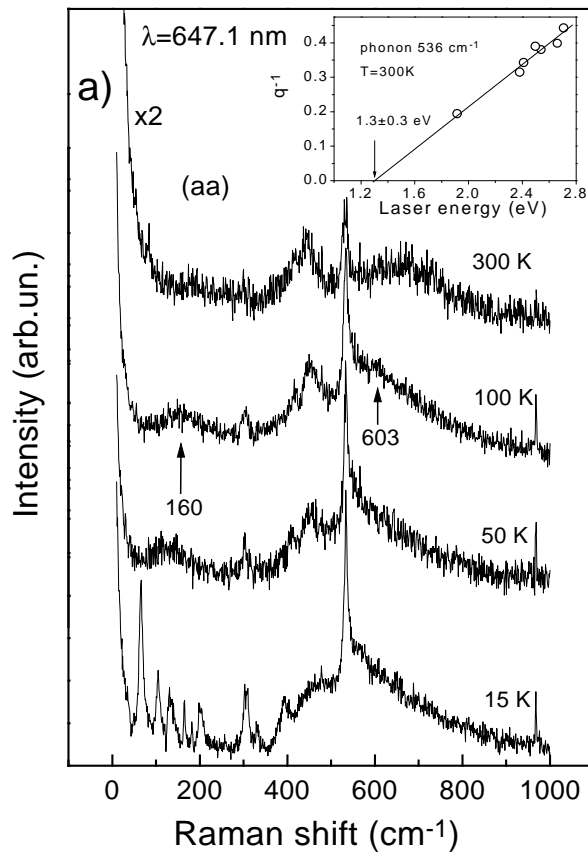
Figure 2. The (aa)-polarized Raman spectra of α'-NaV$_2$O$_5$ single crystal in the temperature range from 15 to 300 K measured with (a) 647.1 nm and (b) 488 nm laser lines. The arrows indicate the central positions of the continua. Inset: a plot of q^{-1} versus excitation frequency as obtained by fitting the line shape of the 536 cm^{-1} phonon mode. The line is computed as described in the text.

atoms are situated between layers as intercalates. This magnetic structure is expected to be truly one dimensional, since the chains carrying the spin are separated by non-magnetic chains along the *b*-axis. However, the most recent structural analysis [11] shows that all vanadium atoms are equivalent and are in a mixed-valence state. Such a crystalline structure, with the appropriate space group *Pmmn*, is also predicted from polarized Raman scattering [12, 13] and NMR [14] measurements. It is shown in figure 1. Nevertheless, due to strong electron correlations the formation of antiferromagnetic Heisenberg chains is still possible [15], even without charge modulation. The formation of an induced zigzag type of charge ordering along the ladders of V ions at low temperatures is also possible [16]. In either case, the 1D description of the NaV_2O_5 compound should be adequate.

In this paper we present and discuss the Raman spectra of $α′$-NaV_2O_5 single crystal. We have assigned the new modes appearing in the low-temperature spectra. The lowest-lying excitation coincides with the magnetic gap estimated by susceptibility measurements, as well as with our numerical result. The onset of the magnetic continuum has also been assigned on the basis of the Monte Carlo simulation, giving reasonable values for the model parameters $δ$ and J. In the paramagnetic phase, continuum-like features have been observed and described as an indication of d–d electronic transitions of V ions.

We argue that our Raman spectra clearly support the charge-ordering phase transition scenario with subsequent formation of one-dimensional magnetic chains.
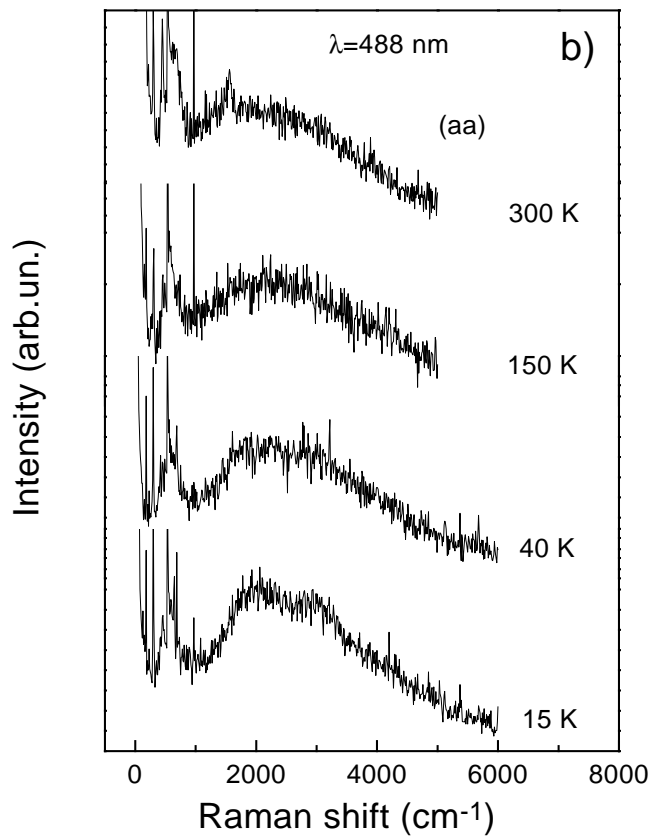
Figure 2. (Continued)

2. Experiment

The single crystals of α'-NaV$_2$O$_5$ with a size of approximately $1 \times 4 \times 0.5$ mm^3, along a-, b- and c-axes, are obtained as described in [1]. Spectral lines of krypton- and argon-ion lasers are used as excitation sources. The light beam with an average power of 100 mW was focused on the sample surface using a cylindrical lens. All of the spectra are obtained in the backscattering geometry. The scattered light was collected with an objective, aperture 1:1.4. The monochromator used was a Jobin–Yvon Model U1000, equipped with a Peltier-effect-cooled RCA 31034 A photomultiplier with a conventional photon-counting system. Temperature was controlled with a closed-cycle helium cryostat (Leybold).

Numerical calculations were carried out on a four-processor Origin 2000 computer, courtesy of Institute of Physics Computer Facilities (IPCF).

3. Raman spectra

The Raman scattering spectra of α'-NaV$_2$O$_5$ at various temperatures between 15 and 300 K are presented in figure 2. The (aa)-polarized spectra are measured using $\lambda = 647.1$ nm (figure 2(a)) and $\lambda = 488$ nm (figure 2(b)) laser lines. The existence of the phase transition and the appearance of new modes are clearly observed in the 15 K spectra. For temperatures higher than the phase transition temperature, $T_{SP} = 34$ K, besides phonons at about 89, 306, 424, 452, 536, 969 cm^{-1}, three broad features centred at 160, 603 and 2400 cm^{-1} ($T = 100$ K) have been observed. Detailed discussion of the phonon mode polarization dependence in the paramagnetic phase is given in [13]. Here we consider only the additional structures. We have observed the continuum-like structures in the (aa)-polarized configuration only. Similar broad features have been observed in infra-red (IR) reflection spectra [13] for $E \parallel a$ as well. The overlap between phonons and continua is analysed on the basis of resonance effects. We have found that the phonon structure at 536 cm^{-1} shows Fano-type asymmetry, indicating a strong interaction with the 603 cm^{-1} continuum. To understand the origin of this broad continuum we have analysed the line shape of the 536 cm^{-1} mode using several laser line energies and fitting to Fano's expression [17]. The fitting parameter q depends on the frequency of scattered light, indicating different frequency dependences for the phonon and continuum scattering processes. Moreover, if the electronic excitation of α'-NaV$_2$O$_5$ can be approximated as the one-dimensional critical point E_0, then q^{-1} is proportional to $\omega_0 - \omega_L$ [18]. From the linear extrapolation of q^{-1} versus excitation frequency (see the inset of figure 2(a)), we have obtained the value $E_0 = 1.3 \pm 0.3$ eV. This value is in very good agreement with the optical absorption band at 1.25 eV, ascribed as arising from d–d electronic transitions of V ions [9]. The asymmetry is also observed for 254 and 505 cm^{-1} IR-active phonons in $E \parallel a$ spectra [13]. On the basis of this asymmetry and the similarities between continua energies in IR and Raman spectra, we suggest that they have the same origin. Accordingly, we have assigned the 603 cm^{-1} (75 meV) Raman continuum as arising from a transition between d-electronic V levels split by the crystal-field effect. We suggest that the two broad bands at 160 and 2400 cm^{-1} (15 and 298 meV) are connected to the other two d–d transitions, while the fourth one lies at energies between 1 and 2 eV, leading to a broad absorption band in this spectral region. The proposed scheme for the d-level splitting in α'-NaV$_2$O$_5$ crystal is presented in figure 3.

The phonon modes at 418 and 452 cm^{-1} show an unusual temperature dependence. The 418 cm^{-1} mode softens when temperature is decreased, in the same manner as the two broad features described above. As temperature is lowered below T_{SP}, the 418 and 452 cm^{-1} phonons form one broad band, indicating a strong coherent effect with the 603 cm^{-1} continuum. Similar behaviour of these two modes is observed when the sodium concentration is decreased [19],
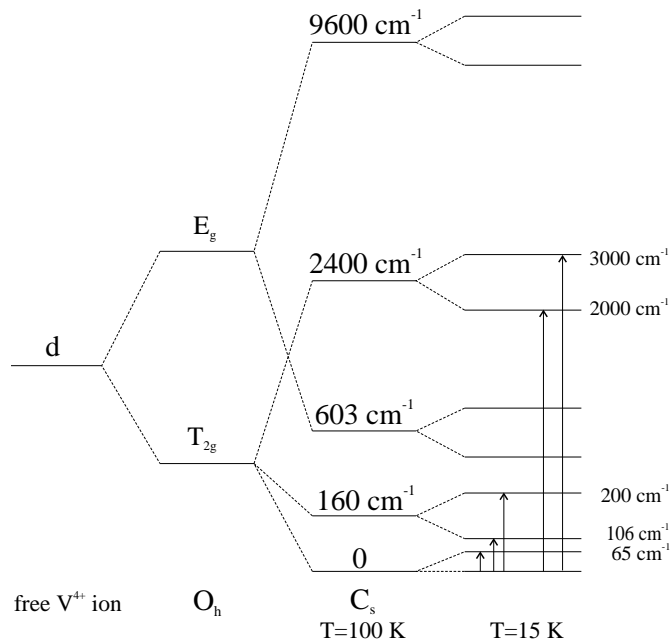
Figure 3. The scheme of d-level splitting in α'-NaV$_2$O$_5$. The transitions observed in the Raman spectra are indicated with arrows.

but the mechanism is not clear at present.

Figure 4 shows the $T = 15$ K Raman spectra for (aa) polarization using three laser line energies. A strong enhancement of low-frequency modes due to the increase of the laser wavelength is found in (aa) polarization only. We will discuss this resonance effect later on.

The polarized Raman spectra measured with the 514.5 nm laser line at the temperature of 15 K are presented in figure 5. The new modes which appear below the transition temperature T_{SP} are indicated. The lowest excitation is observed at 66 cm^{-1}, with the strongest intensity in (ab)-polarized spectra. The onset of the continuum is at 126 cm^{-1}; its magnetic origin is discussed below. The 106 cm^{-1} mode is found to be at its strongest in (bb)-polarized spectra. It is seen that the spectra measured with 647.1 nm laser line (figure 4) differ from the corresponding ones in figure 5. In the latter case, all low-frequency modes have the strongest intensity in (aa) polarization, except the magnetic continuum, which is again observed only with the crossed polarization.

The higher-resolution Raman spectra of the 66 cm^{-1} line for the (aa)-polarized configuration at various temperatures are presented in figure 6(a). We have found this line to consist of two modes with frequencies of about 65 and 67 cm^{-1}. The positions of these modes are obtained by a two-Lorentzian fit to the experimental data. In the same spectra, the 83 cm^{-1} phonon mode is clearly observable. The 65 cm^{-1} mode shifts toward lower energies with increasing temperature (see the left-hand inset in figure 6(a)), while the 67 cm^{-1} mode remains at the same energy. Both structures broaden and disappear above T_{SP} and exhibit linear dependence of the integrated intensity on temperature (see the right-hand inset in figure 6(a)). Such behaviour suggests different origins of these two modes, and we have assigned the 65 cm^{-1} mode as a magnetic gap mode Δ_T, i.e. relating to the transition from the magnetic ground state to the lowest triplet state. The neutron scattering studies and ESR
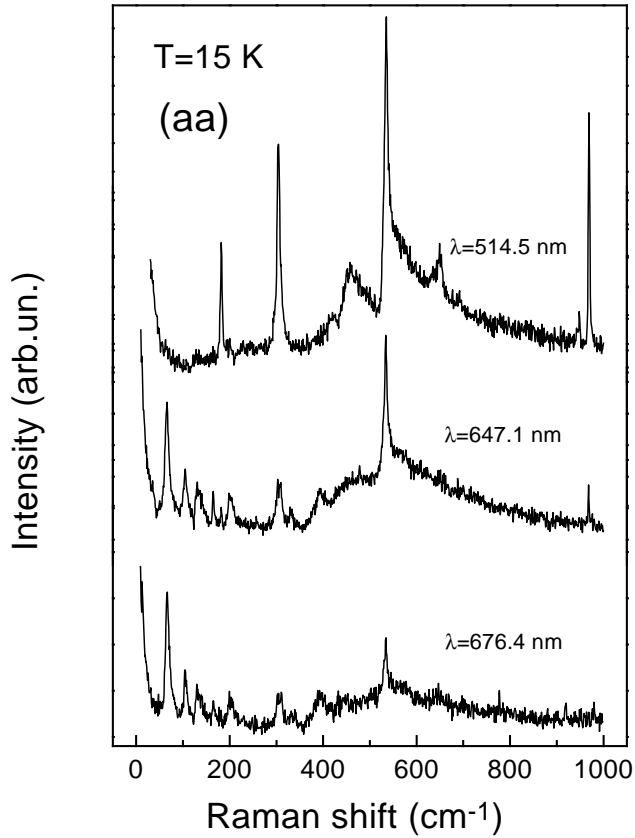
Figure 4. The (*aa*)-polarized Raman spectra of α'-NaV$_2$O$_5$ single crystal measured with different laser line energies at $T = 15$ K.

and susceptibility measurements give spin-gap values around $\Delta_T = 70 \pm 10$ cm^{-1}, which is in a good agreement with our result. The 67 cm^{-1} line probably corresponds to the Brillouin-zone-edge frequency of an acoustic phonon, becoming active due to the doubling of the unit cell in the spin–Peierls phase.

The next thing that we analyse is the continuum observed in (*ab*) polarization as a function of temperature, using the 514.5 nm laser line, in figure 6(b). Again, in (*ab*) polarization, the 66 cm^{-1} mode exhibits a shift of $\sim$3 cm^{-1} toward lower energies when the temperature is increased. A similar shift has been observed for the onset of the magnetic continuum at 126 cm^{-1}. With increasing temperature, this part of the spectrum rapidly loses intensity, completely vanishing above the phase transition temperature. The existence of the continuum is also confirmed by the Fano-type asymmetry of the 177 cm^{-1} phonon, as a consequence of its overlap with the continuum. This asymmetry becomes less pronounced with increasing temperature, and is completely absent from the $T = 30$ K spectrum.

4. Monte Carlo calculation

Here we present the results of numerical calculations based on the Green's function Monte Carlo technique (GFMC) [20]. We have modelled NaV$_2$O$_5$ as a 1D Heisenberg antiferromagnet
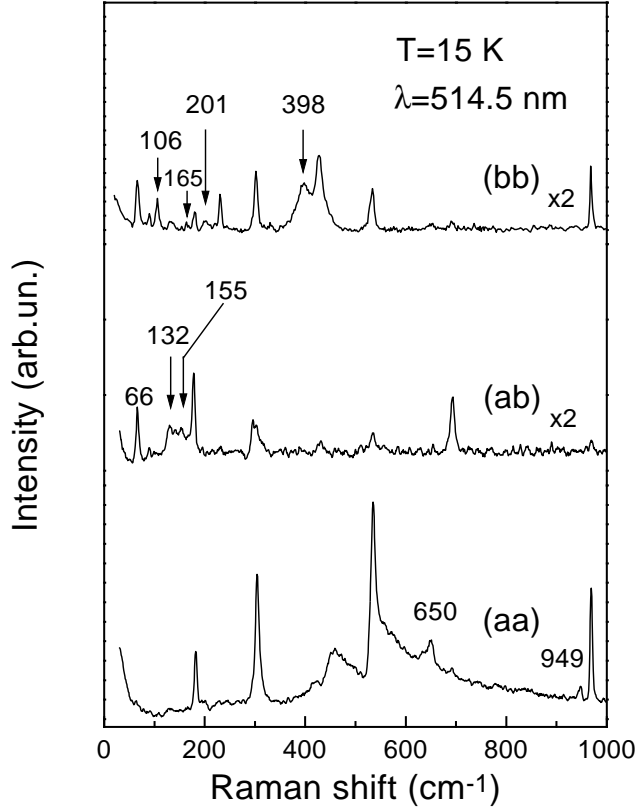
Figure 5. The 15 K Raman spectra in (*bb*), (*ab*) and (*aa*) polarizations, obtained using the 514.5 nm laser line.

with modulated nearest-neighbour coupling and no frustration. This assumption is justified by the susceptibility measurements [8], where the low-temperature behaviour is well described by the Hamiltonian

$$\mathcal{H} = J \sum_{i=1}^{N} (1 + (-1)^i \delta) \vec{S}_i \cdot \vec{S}_{i+1} \tag{1}$$

where the $\vec{S}_i$ are spin-1/2 operators. We have taken periodic boundary conditions, so only rings with even numbers of spins were studied. We have calculated the energies of the ground, the first excited triplet ($S_{tot} = 1$) and the quintuplet ($S_{tot} = 2$) states for rings with $N = 6, 10, 20, 100$ and 200 spins. All of these energies are calculated exactly, with no approximation. The resulting triplet and quintuplet gaps, Δ_T and Δ_Q, are shown in figure 7(a) for $\delta = 0.05$. The extrapolation for $N \to \infty$ is done using the function

$$\Delta_{T,Q}(N) = \Delta_{T,Q} + (A/N + B/N^2 + C/N^3) \exp(-N/N_0).$$

Similar simpler functions have been used in [21] for the extrapolation of gaps obtained by Lanczos diagonalization for systems with $N = 28$ and smaller systems. Here we have chosen a more complicated *ansatz* to fit smaller-N gaps also. The estimated error for the extrapolated values of triplet and quintuplet gaps is less than 1%; the sizes of the symbols in the figures do not represent this error. Further details of the extrapolation procedure can be found in [22].
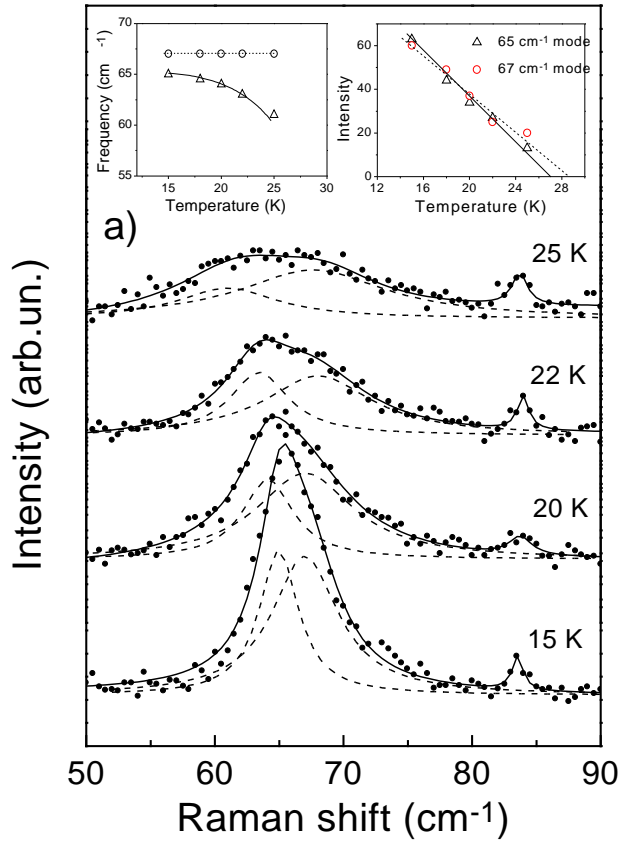
Figure 6. (a) The (aa)-polarized Raman spectra of the $66 \, \mathrm{cm}^{-1}$ feature at various temperatures from 15 to 25 K, obtained using the 647.1 nm laser line. Full curves indicate a fit of the experimental data (circles) to a sum of two Lorentzians (dashed curves). Right-hand inset: the integrated intensity dependences of the 65 and $67 \, \mathrm{cm}^{-1}$ modes as functions of temperature. Left-hand inset: the frequency dependences of the two modes as functions of temperature. The solid curves in the insets are guides to the eye. (b) The Raman spectra of α'-NaV$_2$O$_5$ as a function of temperature in the (ab)-polarized configuration, obtained using the 514.5 nm laser line.

The extrapolated results for all values of δ considered are given in figure 7(b). The singlet–triplet gap is excellently fitted by the simple formula $\Delta_T/J = 2\delta^{3/4}$, $0.01 < \delta < 1$. This has also been found in the recent study [23]. In the limit $\delta \to 1$ this formula coincides with the leading three orders of the perturbation theory result [24]. The $\delta < 0.01$ region is of no concern to us, and we do not know where the crossover to the known [25, 26] critical behaviour $\Delta_T/J \sim \delta^{2/3}/\sqrt{|\ln \delta|}$ occurs.

The singlet–quintuplet gap cannot be fitted in such a simple fashion. We have found it above the double singlet–triplet gap value, at the energy $\Delta_Q = 2\Delta_T + \epsilon$. This is consistent with the findings of the RPA study [27] where this mode was identified as an anti-bound two-magnon state. The 'anti-boundedness' ϵ decreases towards zero when δ goes to 1. According to the estimated error of our calculation, the existence of a quintuplet state at an energy different to $2\Delta_T$ is established for $\delta \leqslant 0.1$ (see the inset in figure 7(b)).
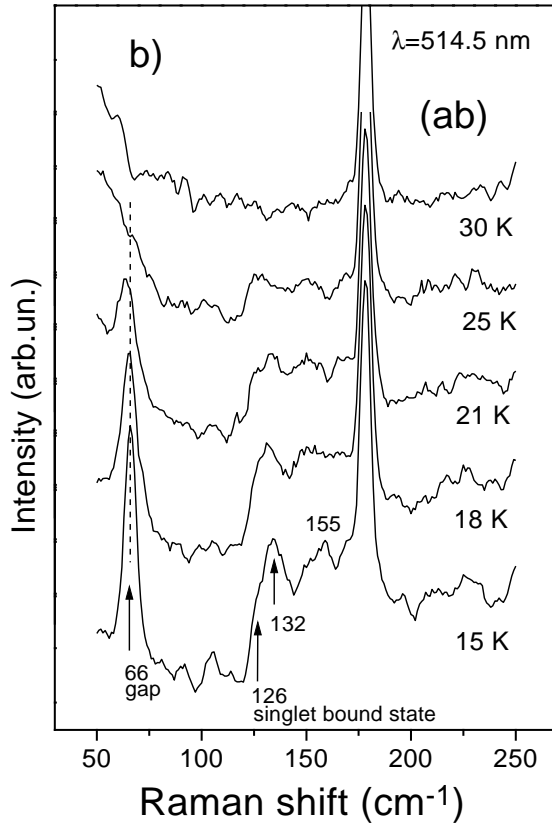
Figure 6. (Continued)

5. Discussion

To begin with, we compare the results of our GFMC calculation with other numerical results. The ground-state energy is in excellent agreement with the Bethe *ansatz* solution [28] in the limit $\delta \rightarrow 0$, and with the results for isolated dimers when $\delta \rightarrow 1$ [24]. Our values for the triplet gap coincide precisely with the exact-diagonalization results [29] as well. The most important point, however, is the exact calculation of the lowest-lying quintuplet state, $S_{tot} = 2$. As already mentioned above, this mode at energy $\Delta_Q = 2\Delta_T + \epsilon$ has been identified as an anti-bound two-magnon state [27]. According to [27] study, one should also expect a singlet two-magnon bound state at energy $\Delta_S = 2\Delta_T - 2\epsilon$. Such an excited singlet state cannot be calculated exactly using the GFMC technique, but it can be estimated using this formula.

The low-temperature susceptibility measurements [8] can be well described by the Bulaevskii theory, indicating the spin–Peierls transition at 34 K. The corresponding values of the exchange integral J and the dimerization δ are $J = 441$ K and $\delta = 0.048$. Using slightly different parameters, $J = 455$ K and $\delta = 0.047$, we have calculated the singlet–triplet and singlet–quintuplet transitions to occur at $\Delta_T = 65$ cm^{-1} and $\Delta_Q = 132$ cm^{-1}. These values are obtained by a linear interpolation between the calculated gaps for $\delta = 0.04$ and $\delta = 0.05$. The singlet–singlet transition at $\Delta_S = 126$ cm^{-1} is obtained using the above estimate, with 'boundedness' $2\epsilon = 4$ cm^{-1}. This value of Δ_S is in good agreement with the
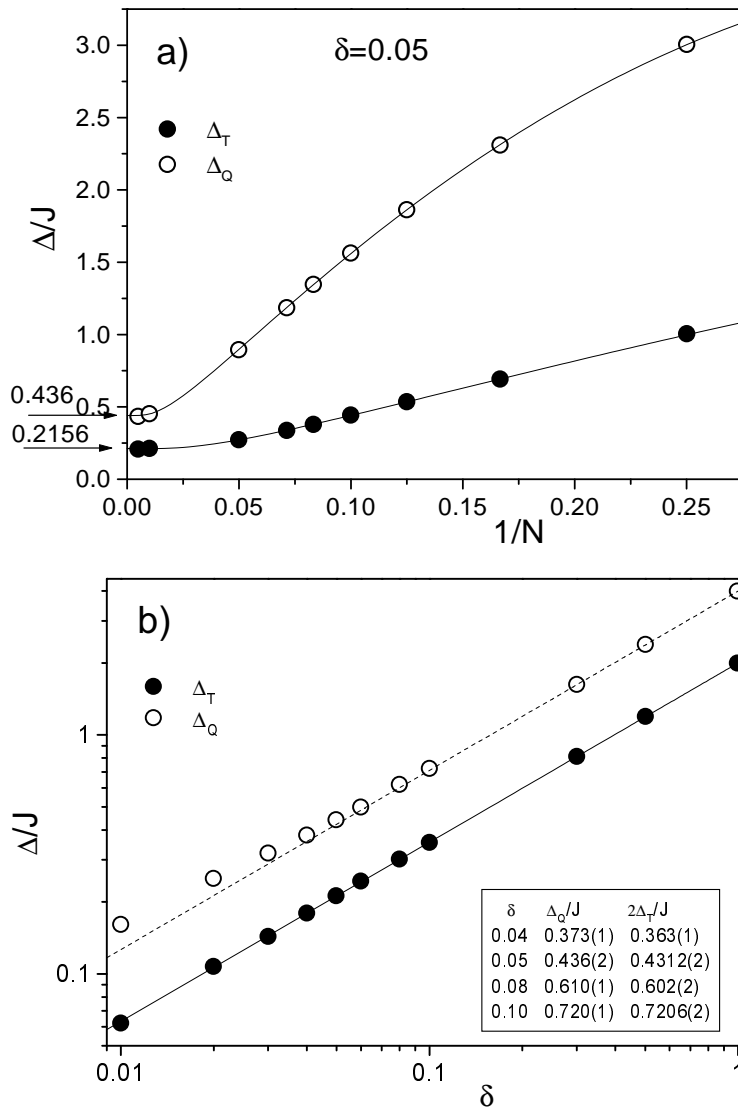
Figure 7. (a) The triplet and quintuplet gaps versus $1/N$, for $\delta = 0.05$. The curves are fitting functions defined in the text. (b) The extrapolated values, $N \to \infty$, for triplet and quintuplet gaps as functions of δ. The full line shows the function $\Delta/J = 2\delta^{3/4}$. The dashed line shows the function $\Delta/J = 4\delta^{3/4}$; see the text. Inset: the gap values with error bars for some values of δ.

exact-diagonalization study [21], which gives a singlet-to-triplet gap ratio of $\sim$1.9.

Next, we discuss the nature of the 65 cm^{-1} feature in the Raman spectra. The value of 65 cm^{-1} coincides with our numerical result for the triplet gap and it is plausible that the mode at this position arises from a one-magnon scattering process. The energy of this mode is in agreement with other measurements of the spin gap. Moreover, it shifts toward lower values with increasing temperature and decreasing sodium concentration [19]. Sodium deficiency strongly suppresses the SP transition [30], giving an additional proof of the magnetic origin of this mode. At present, the behaviour of the 65 cm^{-1} mode in a magnetic field remains to

be studied. Some preliminary results show that it does not change in fields of up to 7 T [31]. However, the presence of the 67 cm^{-1} feature may inhibit the one-magnon mode splitting in a magnetic field.

Let us now consider the continuum starting at 126 cm^{-1}. Its onset coincides with the singlet–singlet excitation Δ_S found in our GFMC calculation, indicating its magnetic origin [32]. The appearance of the continuum in (ab) polarization suggests that either the dimerized chains are not formed along the b-direction, or the exchange scattering mechanism of Fleury and Loudon [33] is not applicable in this case.

Now, we discuss the other low-temperature modes. Below the transition temperature, the single-ion levels split due to exchange interaction between V ions. In this case, the lowest paramagnetic band observed at around 160 cm^{-1} ($T = 100$ K) gives three transitions in the antiferromagnetic phase at 65, 106 and 200 cm^{-1} (figure 3). As we have already mentioned, the first one corresponds to a one-magnon scattering process while the others correspond to higher-energy excitons. The 132 cm^{-1} feature relates to a second-order process coming from the 66 cm^{-1} mode, and may contain two-phonon 134 cm^{-1} and two-magnon 130 cm^{-1} modes. When temperature is increased, the 165 cm^{-1} mode does not broaden as much as the other modes for the same polarization do, and we believe that this is an edge phonon. New exciton modes arising from the splitting of high-temperature paramagnetic bands are observed at frequencies of 2000 and 3000 cm^{-1} (figure 2(b)). All of these modes are enhanced when the red laser light is used as the excitation source, since its light energy is near the 1.25 eV absorption band. This supports the assumption that Raman spectra show excitons.

Finally, it is interesting to compare our results with those for $CuGeO_3$, the first inorganic material found to exhibit the spin–Peierls transition. The excitation from the ground to the first triplet state, corresponding to the gap energy, is not observed in the Raman spectra of $CuGeO_3$ [34]. This is a consequence of the spin–orbit interaction, responsible for the light scattering mechanism and magnon excitation, being too small in Cu^{2+} ions. The magnetic mode at 30 cm^{-1} observed for $CuGeO_3$ is described as an excitation from the ground state to the singlet state [34–36]. For NaV_2O_5 we have found both one-magnon excitation and a singlet–singlet transition, at 65 and 126 cm^{-1}. The broad magnon band, centred at about twice the maximum magnon energy, found for $CuGeO_3$ [34], is not observed in our NaV_2O_5 Raman spectra. This is consistent with the assumption that frustration is negligible in this material.

The existence of the magnetic continuum above the SP transition temperature is not confirmed by our data, suggesting a phase transition character for NaV_2O_5 different to that for $CuGeO_3$. In the latter case, the spin-wave continuum in the high-temperature phase is well described by the uniform Heisenberg model [34]. For such a system, spin fluctuations appear in the Raman spectra as a broad feature centred at $2.7J$. In the charge-ordering phase transition scenario, the rapid electron oscillations between vanadium sites at high temperatures make the observation of spin fluctuations difficult. Hence we believe that our Raman spectra clearly support a charge-ordering nature for the phase transition in NaV_2O_5.

To conclude, we have found that paramagnetic phase Raman spectra of NaV_2O_5 exhibit, besides phonon modes, d–d electronic transitions of V ions, as a consequence of crystal-field d-level splitting. At temperatures below $T_{SP} = 34$ K the crystal undergoes a charge-ordering phase transition to an antiferromagnetic phase, described by the one-dimensional dimerized Heisenberg model without frustration. Due to magnetic interaction, spin degeneracy is removed, and we have observed exciton modes in the low-temperature Raman spectra. The lowest-frequency mode has been assigned as corresponding to a one-magnon scattering process. Its energy is in good agreement with the gap estimation obtained from susceptibility measurements and with our numerical result as well. The Monte Carlo calculation has also led to the assigning of the magnetic continuum onset, giving reasonable values for δ and J.

Acknowledgments

References

 [1] Isobe M and Ueda Y 1996 *J. Phys. Soc. Japan* **65** 1178
 [2] Hase M, Terasaki I and Uchinokura K 1993 *Phys. Rev. Lett.* **70** 3651
 [3] Fujii Y, Nakao H, Yosihama T, Nishi M, Nakajima K, Kakurai K, Isobe M, Ueda Y and Sawa H 1997 *J. Phys. Soc. Japan* **66** 326
 [4] Ohama T, Isobe M, Yasuoka H and Ueda Y 1997 *J. Phys. Soc. Japan* **66** 545
 [5] Vasil'ev A N, Smirnov A I, Isobe M and Ueda Y 1997 *Phys. Rev.* B **56** 5065
 [6] Popova M N, Sushkov A B, Vasil'ev A N, Isobe M and Ueda Y 1997 *Pis. Zh. Eksp. Teor. Fiz.* **65** 711
 [7] Smirnov D, Millet P, Leotin J, Poilblanc D, Riera J, Augier D and Hansen P 1998 *Phys. Rev.* B **57** R11 035
     (Smirnov D, Millet P, Leotin J, Poilblanc D, Riera J, Augier D and Hansen P 1998 *Preprint* cond-mat/9801194)
 [8] Weiden M, Hauptmann R, Geibel C, Steglich F, Fischer M, Lemmens P and Güntherodt G 1997 *Z. Phys.* B **103** 1
 [9] Golubchik S A, Isobe M, Ivlev A N, Mavrin B N, Popova M N, Sushkov A B, Ueda Y and Vasil'ev A N 1997 *J. Phys. Soc. Japan* **66** 4042
[10] Carpy A and Galy J 1982 *Acta Crystallogr.* B **31** 1481
[11] von Schnering H-G, Grin Yu, Kaupp M, Somer M, Kremer R, Jepsen O, Chatterji T and Weiden M 1998 *Z. Kristallogr.* **246** at press
[12] Lemmens P, Fischer M, Els G, Güntherodt G, Mishenko A S, Weiden M, Hauptmann R, Geibel C and Steglich F 1998 *Phys. Rev.* B **58** 14 159
[13] Popović Z V, Konstantinović M J, Gajić R, Popov V N, Raptis Y S, Vasil'ev A N, Isobe M and Ueda Y 1998 *J. Phys.: Condens. Matter* **10** L513
[14] Ohama T, Yasuoka H, Isobe M and Ueda Y 1999 *Phys. Rev.* B **59** at press
[15] Horsch P and Mack F 1998 *Eur. Phys. J.* B **5** 367
     (Horsch P and Mack F 1998 *Preprint* cond-mat/9801316)
[16] Seo H and Fukuyama H 1998 *J. Phys. Soc. Japan* **67** 2602
     (Seo H and Fukuyama H 1998 *Preprint* cond-mat/9805185)
[17] Fano U 1961 *Phys. Rev.* **124** 1866
[18] Cerdeira F, Fjeldly T A and Cardona M 1973 *Phys. Rev.* B **8** 4734
[19] Konstantinović M J, Fischer M, van Loosdrecht P H M, Güntherodt G, Popović Z V, Vasil'ev A N, Isobe M and Ueda Y 1999 to be published
[20] Trivedi N and Ceperley D M 1990 *Phys. Rev.* B **41** 4552
[21] Augier D, Poilblanc D, Haas S, Delia A and Dagotto E 1997 *Phys. Rev.* B **56** R5732
[22] Ladavac K and Belić A 1999 to be published
[23] Barnes T, Riera J and Tennant D A 1998 *Preprint* cond-mat/9801224
[24] Harris A B 1973 *Phys. Rev.* B **7** 3166
[25] Cross M C and Fischer D 1979 *Phys. Rev.* B **19** 402
[26] Black J L and Emery V J 1981 *Phys. Rev.* B **23** 429
[27] Uhrig G S and Schulz H J 1996 *Phys. Rev.* B **54** R9624
[28] Yang C N and Yang C P 1966 *Phys. Rev.* **150** 327
[29] Soos Z G, Kuwajima S and Mihalick J E 1985 *Phys. Rev.* B **32** 3124
[30] Isobe M and Ueda Y 1997 *J. Alloys Compounds* **262–263** 180
[31] Els G 1998 Private communication
[32] Bonner J C and Blöte H W J 1982 *Phys. Rev.* B **25** 6959
[33] Fleury P A and Loudon R 1968 *Phys. Rev.* **166** 514
[34] van Loosdrecht P H M, Boucher J P and Martinez G 1996 *Phys. Rev. Lett.* **76** 311
[35] Kuroe H, Sekine T, Hase M, Sasago Y, Uchinokura K, Kojima H, Tanaka I and Shibuya Y 1994 *Phys. Rev.* B **50** 16 468
[36] Lemmens P, Fischer M, Güntherodt G, Gros C, van Dongen P G J, Weiden M, Richter W, Geibel C and Steglich F 1997 *Phys. Rev.* B **55** 15 076